Electronic Supplementary Information (ESI)

Ligand ordering determines the catalytic response of hybrid palladium nanoparticles in hydrogenation

Davide Albani,[a] Gianvito Vilé,[a] Sharon Mitchell,[a] Peter T. Witte,[b] Neyvis Almora-Barrios,[c] René Verel,[a] Núria López,*[,c] and Javier Peréz-Ramírez*[,a]

[a] Institute for Chemical and Bioengineering, Department of Chemistry and Applied Biosciences, ETH Zurich, Vladimir-Prelog-Weg 1, 8093 Zurich, Switzerland.

[b] BASF Nederland BV, Strijkviertel 67, 3454 De Meern, The Netherlands.

[c] Institute of Chemical Research of Catalonia (ICIQ) and Barcelona Institute of Technology (BIST), Av. Països Catalans 16, 43007 Tarragona, Spain.

*Corresponding authors. E-mails: nlopez@iciq.es (N.L.); jpr@chem.ethz.ch (J.P.R.)

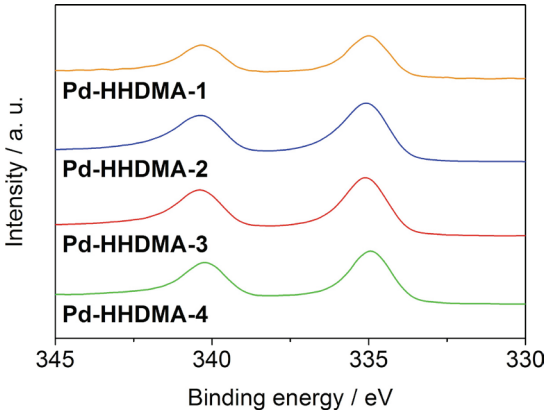

Figure S1. Pd 3*d* core level X-ray photoelectron spectroscopy of the catalysts.

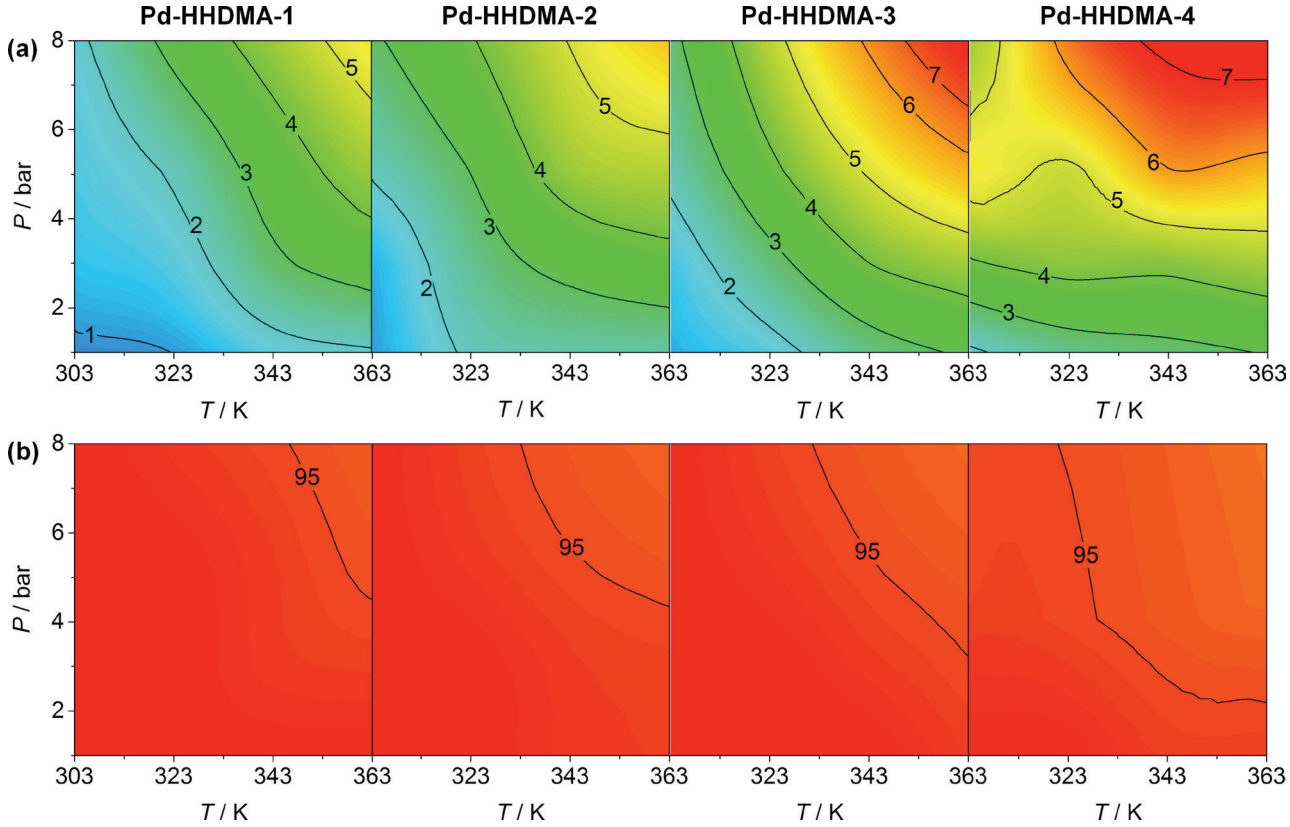

Figure S2. Reaction rate (in 10^3 h^{-1}, a) and selectivity to *cis*-3-hexene (in %, b) in the hydrogenation of 3-hexyne. Conditions: W_{cat} = 0.1 g, F_L(3-hexyne+toluene) = 1 cm^3 min^{-1}, $F_G(H_2)$ = 36 cm^3 min^{-1}. The contour maps were obtained through spline interpolation of 16 experimental points.

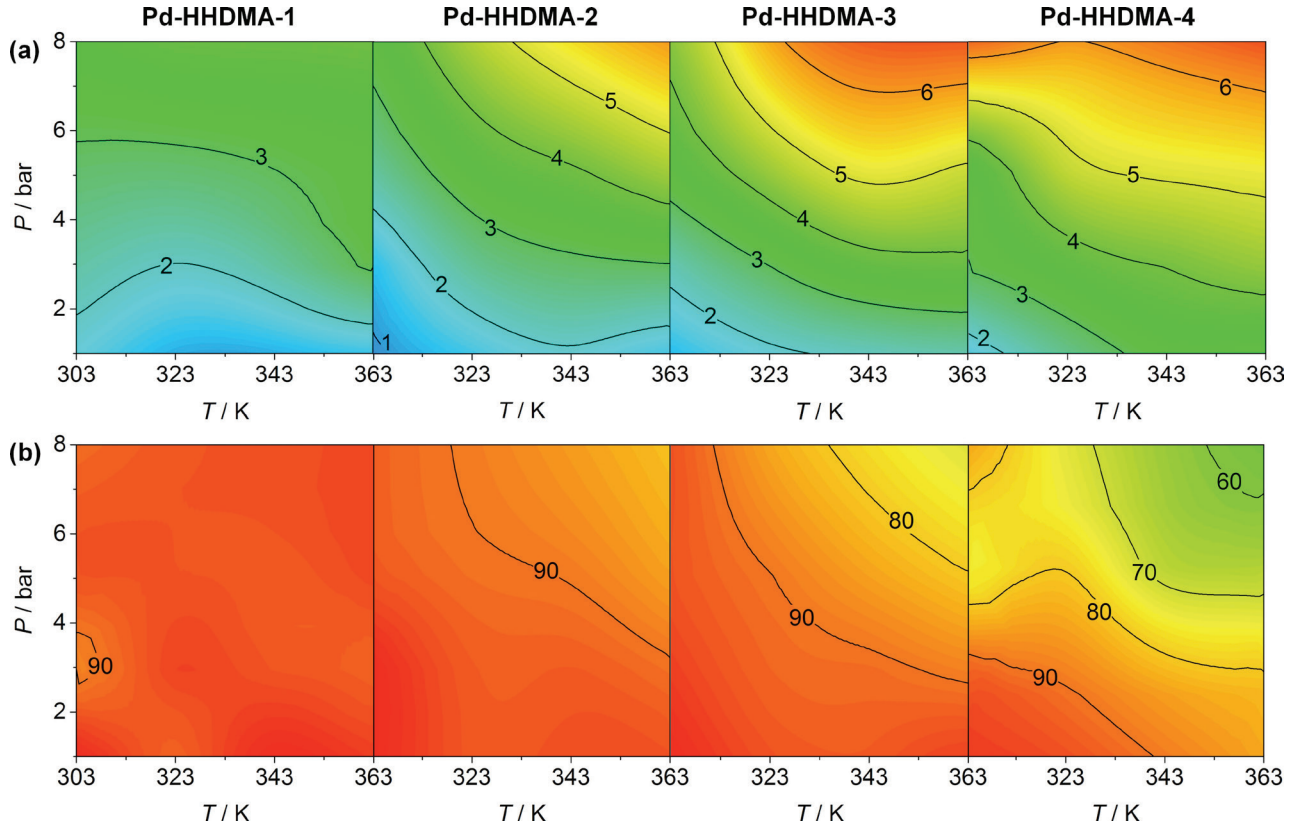

Figure S3. Reaction rate (in 10^3 h^{-1}, a) and selectivity to 2-methyl-3-buten-2-ol (in %, b) in the hydrogenation of 2-methyl-3-butyn-2-ol. Conditions: W_{cat} = 0.1 g, F_L(2-methyl-3-butyn-2-ol+toluene) = 1 cm^3 min^{-1}, $F_G(H_2)$ = 36 cm^3 min^{-1}. The contour maps were obtained through spline interpolation of 16 experimental points.

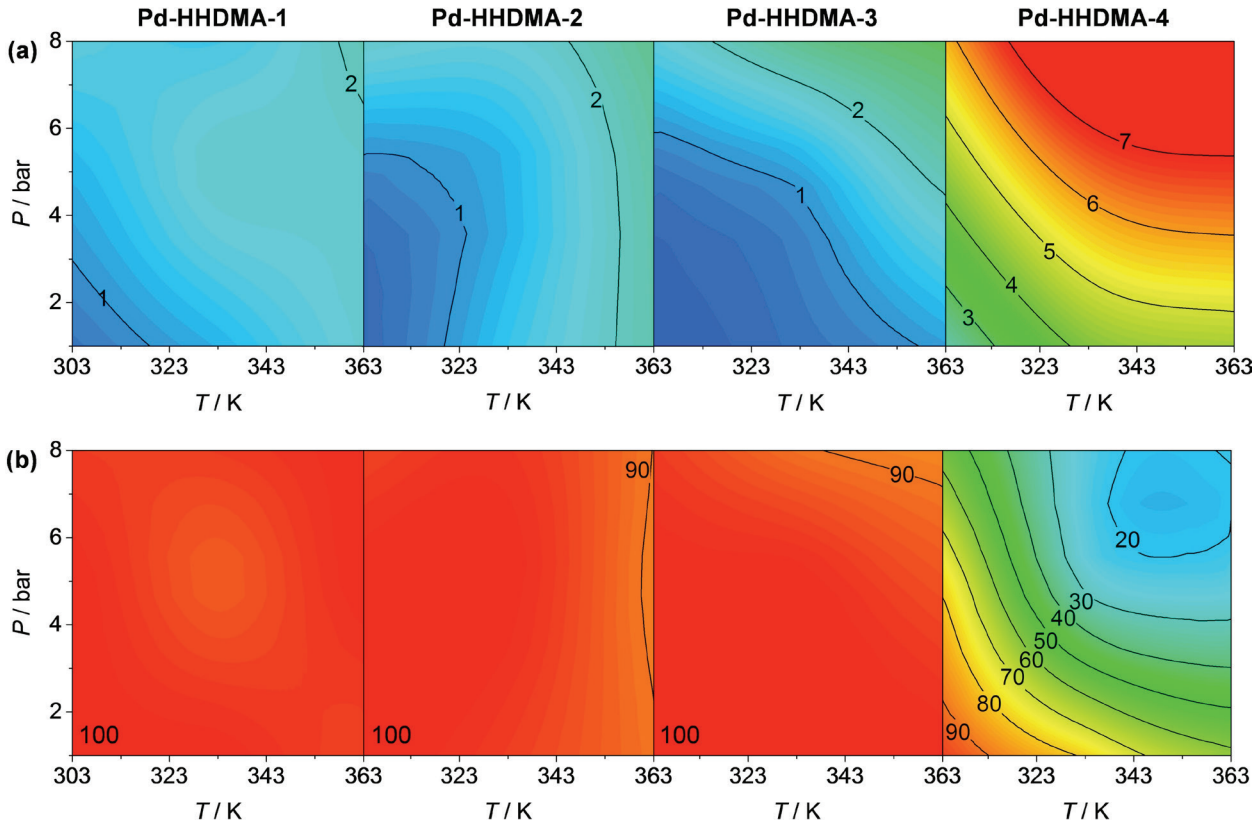

Figure S4. Reaction rate (in 10^3 h^{-1}, a) and selectivity to 1-hexene (in %, b) in the hydrogenation of 1-hexyne. Conditions: W_{cat} = 0.1 g, F_L(1-hexyne+cyclohexane) = 1 cm^3 min^{-1}, $F_G(H_2)$ = 36 cm^3 min^{-1}. The contour maps were obtained through spline interpolation of 16 experimental points.

To confirm the influence of the solvent, the hydrogenation performance of the catalysts was investigated in both toluene and cyclohexane. Consistent with the findings in the main manuscript, comparison of Figures 5 and S4 reveal an increased activity and a decreased product selectivity with increasing HHDMA concentration. This effect is more prominent in the case of cyclohexane due to the bulkier nature of cyclohexane as compared to toluene, leading to different conformation of the ligand chains, as well as to the differing hydrogen solubility observed in this solvent.[1,2] In fact, in cyclohexane at low HHDMA content, the ligand produces lower H concentration on the metal surface resulting in a lower activity, whereas at higher HHDMA concentrations, the solvent molecules interlock with the fully extended chains hindering the transport of the semi-hydrogenated products. Correspondingly, the larger residence time on the surface increases the probability of over-hydrogenation and isomerisation.

Additional details on the determination of the order parameter. In a large $p(10\times10)$ unit cell (surface dimensions around 28×28 Å^2), variable amounts of ligand were adsorbed on the surface in order to attain coverages of 0.05, 0.10, 0.18, 0.25 ML, corresponding to 5, 10, 18, and 25 HHDMA molecules per unit cell. The simulated systems were equilibrated for 100 ps, using the DL_POLY classical Molecular Dynamics[3] at 303 K under constant number-volume-temperature conditions.[3] The Verlet algorithm[4] was used to integrate the equations of motion of the particles, using a time step of 1 fs; the temperature, on the other hand, was constrained using the Nosé-Hoover thermostat.[5,6] The potential model for Pd metal and HHDMA molecules was taken from earlier works.[7] The final configurations from classical Molecular Dynamics were assumed as initial structures and re-optimised following our Density Functional Theory scheme.

Figure S5 shows the structure expected at a high HHDMA coverage on the Pd(111) surface (0.25 ML). θ_i, in particular, is the angle formed between the i^{th} molecular axis of the ligand and the normal to the surface, while θ_j is the angle formed between the j^{th} molecular axis of the ligand and the normal to the surface.[8,9] These angles can range between 0° and 90°. At 0.25 ML coverage, $\theta_i = 34°$, and $\theta_j = 0°$. In our case, the order parameter, S_{HHDMA}, is determined by measuring the angles, θ_i, over the time and averaging them to the total number of ligand molecules in the simulation box.

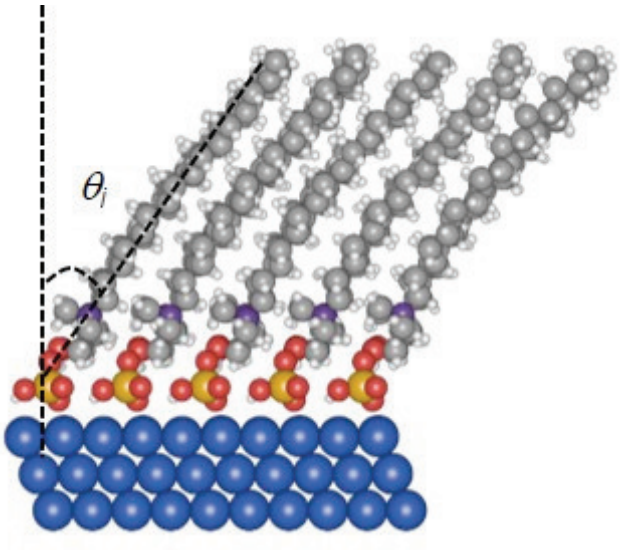

Figure S5. Representation of the self-assembled monolayer of HHDMA supported on Pd(111).

The fitting in Figure 9b of the main manuscript was performed using the Michaelis-Menten interpolation of theoretical points, applying the following equation:

$$S_{HHDMA} = \frac{(1.43 \pm 0.21)([P/Pd_{surf}] - [P/Pd_{surf}]_0)}{(0.03 \pm 0.02) + ([P/Pd_{surf}] - [P/Pd_{surf}]_0)}$$

The obtained regression factor was 0.94. Figure S6 shows the correlation between the normalised reaction rate (r/r_0, where r_0 corresponds to the rate over the catalyst with the minimal surfactant coverage), the order parameter,

S_{HHDMA}. A quasi-linear relationship is observed for all the investigated substrates (see the fitting parameters in Table S1).

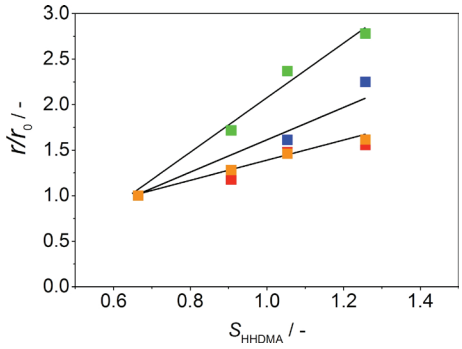

Figure S6. Relative reaction rate as a function of the order parameter, S_{HHDMA}, in the hydrogenation of 1-hexyne (orange), 3-hexyne (green), 2-methyl-3-butyn-2-ol (blue), and 4-octyne (red).

Table S1. Parameters retrieved from the linear fitting in Figure S6.

Reactant	***a* / -**	***b* / -**	r^2 **/ -**
1-hexyne	3.10±0.30	−1.04±0.28	0.98
3-hexyne	1.01±0.19	0.33±0.19	0.90
2-methyl-3-butyn-2-ol	2.00±0.40	−0.40±0.40	0.93
4-octyne	1.05±0.08	0.32±0.08	0.98

The linear fitting was performed using the following equation:

$$\frac{r}{r_0} = aS_{HHDMA} + b$$

Examination of Figure 9c of the main manuscript and Table S1 indicates that S_{HHDMA} is the main intrinsic descriptor of the catalytic activity, since a linear correlation is found for each substrate. The minor differences appearing with different reactants relate to specific catalyst-reactant pair. Thus, internal triple C-C bonds in 3-hexyne and 4-octyne follow the same dependence due to their similar chemical functionality. For dense layers, a significant rearrangement of the molecule is needed, suggesting that molecules containing internal triple bonds may benefit from a 2D (Lindlar-like) configuration. In contrast, dense layers preorient the terminal alkyne functionality, as shown by the highest slope of 1-hexyne. An intermediate behaviour is observed for 2-methyl-3-butyn-2-ol, due to the additional interaction that can occur either to the phosphate head groups or to the side alcohol chain in the quaternary N (H-bonding). Notice that the variations in rate evidenced in different solvents (Figure 5 in the main manuscript and Figure S4) will appear as an extra variable in the rate expression and further alter the *r versus* S_{HHDMA} relationship.

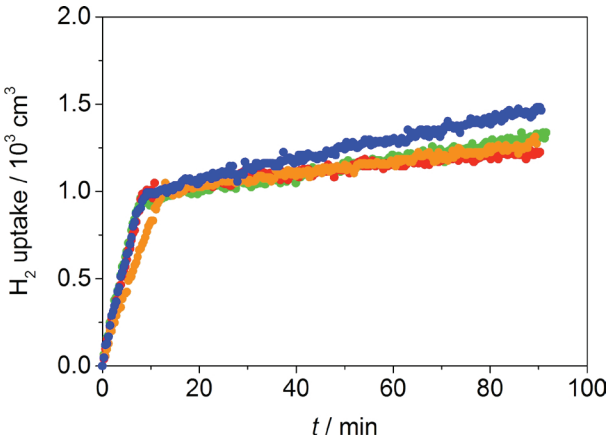

Figure S7. Hydrogen uptake (in 10^3 cm^3) *vs* time (min) in the hydrogenation of 3-hexyn-1-ol over Pd-HHDMA-1 (red), Pd-HHDMA-2 (blue), Pd-HHDMA-3 (green), and Pd-HHDMA-4 (orange). Condition: W_{cat} = 0.4 g, T = 303 K, $P(H_2)$ = 3 bar.

To confirm the selective properties of the ligand-modified catalysts at high degrees of alkyne conversion, the hydrogenation of 3-hexyn-1-ol was performed in a batch reactor. Examination of Figure S7 shows that the reaction kinetics is monitored by the hydrogen uptake. Particularly, all the curves present a similar profile, which is composed of two different parts. Below 10 min of reaction time, the lines have a steep slope, representing the hydrogenation of 3-hexyn-1-ol to cis-3-hexen-1-ol. After 10 min of reaction time, the hydrogen consumption is characterised by with a much more modest slope, indicating over-hydrogenation of cis-3-hexen-1-ol to 1-hexanol. Overall, by comparing the catalysts at 95% of alkyne conversion, the alkene selectivity is around 90-95%, evidencing the intrinsically selective behaviour of the materials.

References

[1] M. W. Cook, D. N. Hanson, B. J. Alder, *J. Chem. Phys.* 1957, **26**, 748.

[2] J. H. Dynond, *J. Phys. Chem*. 1967, **71**, 1829.

[3] I. T. Todorov, W. Smith, K. Trachenko, M. T. Dove, *J. Mater. Chem.* 2006, **16**, 1911.

[4] L. Verlet, *Phys. Rev.* 1967, **159**, 98.

[5] S. Nose, *J. Chem. Phys.* 1984, **81**, 511.

[6] W. G. Hoover, *Phys. Rev. A* 1985, **31**, 1695.

[7] G. Vilé, N. Almora-Barrios, S. Mitchell, N. López, J. Pérez-Ramírez, *Chem. Eur. J.* 2014, **20**, 5926.

[8] A. R. Leach, *Molecular Modelling Principles and Applications*, 2nd ed., Pearson Education, 2001, p. 395.

[9] J. C. Love, L. A. Estroff, J. K. Kriebel, R. G. Nuzzo, G. M. Whitesides, *Chem. Rev.* 2005, **105**, 1103.